PHYSICAL REVIEW B **81**, 184206 (2010)

Surface order in cold liquids: X-ray reflectivity studies of dielectric liquids and comparison to liquid metals

Sudeshna Chattopadhyay,[1] Ahmet Uysal,[1] Benjamin Stripe,[1] Steven Ehrlich,[2] Evguenia A. Karapetrova,[3] and Pulak Dutta[1]
[1]*Department of Physics & Astronomy, Northwestern University, Evanston, Illinois 60208, USA*
[2]*National Synchrotron Light Source, Brookhaven National Laboratory, Upton, New York 11973, USA*
[3]*Advanced Photon Source, Argonne National Laboratory, Argonne, Illinois 60439, USA*
(Received 10 March 2010; published 17 May 2010)

Oscillatory surface-density profiles (layers) have previously been reported in several metallic liquids, one dielectric liquid, and in computer simulations of dielectric liquids. We have now seen surface layers in two other dielectric liquids, pentaphenyl trimethyl trisiloxane, and pentavinyl pentamethyl cyclopentasiloxane. These layers appear below $T \sim 285$ K and $T \sim 130$ K, respectively; both thresholds correspond to $T/T_c \sim 0.2$ where T_c is the liquid-gas critical temperature. All metallic and dielectric liquid surfaces previously studied are also consistent with the existence of this T/T_c threshold, first indicated by the simulations of Chacón *et al.* [Phys. Rev. Lett. **87**, 166101 (2001)]. The layer width parameters, determined using a distorted-crystal fitting model, follow common trends as functions of T_c for both metallic and dielectric liquids.

DOI: 10.1103/PhysRevB.81.184206 PACS number(s): 64.70.kj, 68.03.Hj

I. INTRODUCTION

Liquid-vapor interfaces are ubiquitous in everyday life, and basic features such as surface tension and capillary waves are familiar to most undergraduates. The familiar picture of the free surface, in which the density varies monotonically from that of the liquid to that of the gas, was proposed in 1831 by Poisson[1] as an improvement over an unphysical step-function profile. However, predictions of oscillatory (layered) interfacial density profiles have repeatedly appeared in the literature.[2] The problem is that these predictions were not experimentally confirmed in most liquids. X-ray reflectivity studies, of, e.g., liquid helium,[3] alkanes,[4] ethanol,[5] polymers and polymer solutions,[6,7] water,[8,9] etc., saw only monotonic surface profiles. (All except liquid helium were studied at or near room temperature.)

On the other hand, Rice and co-workers[10,11] proposed that liquid-metal surfaces would be layered because of the role of the electron gas in creating an abrupt transition between the conducting liquid and nonconducting vapor, resulting in an effective "hard wall." This prediction was also not immediately confirmed, but starting some years later, a series of x-ray experiments[12–16] have clearly shown that many liquid metal–vapor interfaces are layered at or above room temperature.

The conclusion implied by the experimental correlation, and supported by the theoretical prediction, is that conduction electrons *cause* surface layering. However, computer simulations of point particle liquids with no electron gas, by Chacon *et al.*[17,18] and by Li and Rice,[19] also showed surface layers at sufficiently low temperatures. When cooled, Lennard-Jones liquids freeze before developing surface layers, but if the interparticle potential is made wide and shallow, this lowers the triple point and/or raises the liquid-gas critical temperature (T_c). Onset of layering in the simulations[17] occurred at $\sim 0.2T_c$.

Shallow and longer-range interatomic potentials are appropriate for liquid metals because of screening by conduction electrons. Indeed, liquid metals tend to have very high T_c. Liquid-metal experiments showing layers were conducted at or above room temperature but invariably well below $0.2T_c$. It is generally impractical to do experiments above $0.2T_c$ in these materials because T_c is so high. The molecular liquid studies that showed no layers were also conducted near room temperature, but this is above $0.2T_c$ (in fact, generally above $0.45T_c$) for these materials. Cooling, would not have helped: most dielectric liquids freeze before $0.2T_c$ can be reached.

Thus all existing observations are technically consistent with the $0.2T_c$ threshold. The prospect of a common picture of layering in all liquids is attractive, although the computer simulations provide no explanation, only empirical evidence. Moreover, the threshold prediction cannot be fully verified in most metallic or dielectric liquids since these can be studied either above or below the purported threshold but not both. The single exception prior to the present work is tetrakis(2-ethylhexoxy)silane (TEHOS), which remains liquid in the bulk at the threshold temperature and clearly shows surface layers developing when cooled to $\sim 0.23T_c$.[20,21]

In this paper, we use "cold liquid" to mean any liquid that is at or below $\sim 0.2T_c$ but is still a bulk fluid and not a solid or glass. We will describe in detail our studies of the surface profiles of two other cold liquids, pentaphenyl trimethyl trisiloxane (PPTMTS),[22] and pentavinyl pentamethyl cyclopentasiloxane (PVPMCPS). The critical temperature for TEHOS is 950 K; that for PPTMTS is significantly higher (~ 1210 K) and that for PVPMCPS is significantly lower (~ 750 K). Nonetheless, these materials have very similar surface-layering behavior. Moreover, the layers in these three dielectric liquids and in several liquid metals show common trends as functions of T_c.

II. EXPERIMENTAL DETAILS AND DATA FITTING

Liquid PPTMTS and PVCMPS were purchased from GELEST, Inc., with a purity of >95% and used as supplied. Molecules of the two liquids are shown in Fig. 1. Figure 1(a)

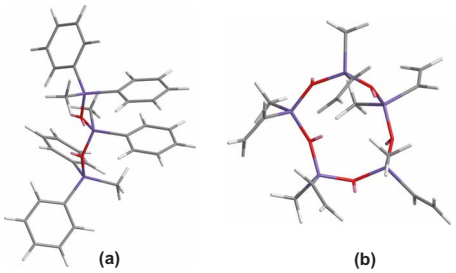

FIG. 1. (Color online) Molecular structure using CHEM3D software: (a) PPTMTS; (b) PVPMCPS.

shows the PPTMTS molecule, consisting of three Si atoms connected to each other through two oxygen atoms, and each Si is also attached to benzene rings and methyl groups so as to form a roughly spheroidal shape (dimensions ~10.5 Å max to ~7.5 Å min). The PVPMCPS molecule is shown in Fig. 1(b). It has a cyclic structure consisting of five Si atoms connected to each other through five oxygen atoms, and each Si is attached to vinyl and methyl groups, again forming a roughly spheroidal shape (dimensions ~9 Å max to ~7.5 Å min).

The dielectric liquid PPTMTS is commercially available as a diffusion-pump oil (Dow Corning 705). Obviously it has a low vapor pressure, which implies a high boiling point and high critical temperature. Further, it means that liquid-films wetting solid substrates can be studied without special precautions to retard evaporation. Its boiling point is ~523 K at 100 Pa;[23] using the Clausius-Clapeyron equation to estimate the normal boiling point, and then using the normal boiling point to estimate the critical temperature,[24] we find that T_c is ~1210 K (this estimation process has an uncertainty of roughly ±5%). The normal boiling point of PVPMCPS is ~535 K (from Gelest catalog) and the estimated critical temperature is ~750 K.

We have measured the surface tension (γ) as a function of temperature (T) using a Wilhelmy-plate method in the range 265–298 K, extrapolated the data,[25] and used this to calculate the interface width due to capillary waves, σ_{cw}.[5,26,27] In Fig. 2, upper panel, measured values of surface tension (open circles) are plotted vs T, and the T dependence fitted using the theoretical expression:[25] $\ln(\gamma)=A+n\ln(T_c-T)$, where T_c is 1210 K for PPTMTS and 750 K for PVPMCPS. A and n are constants determined from best fitting. The surface tension is then extrapolated to lower temperatures, where it cannot be directly measured. The lower panel of Fig. 2 shows σ_{cw}^2 derived from the extrapolated surface tension.

In order to easily cool the liquids in a standard closed-cycle refrigerator and orient their surfaces in a standard diffractometer, PPTMTS and PVCMCPS were studied in the form of thin-films wetting solid substrates.[20] Uniform liquid films of PPTMTS of thickness ~15 000 Å were obtained by spreading the liquid on silicon substrates by spin coating. The viscosity of PVCMCPS is low, and therefore uniform liquid films of thickness ~5000 Å were prepared simply by putting a few drops of liquid on the substrate, allowing the liquid to spread, and then draining the excess.[20,21] For one film of PPTMTS, we used the same sample preparation method as PVPMCPS, and we saw no differences in x-ray

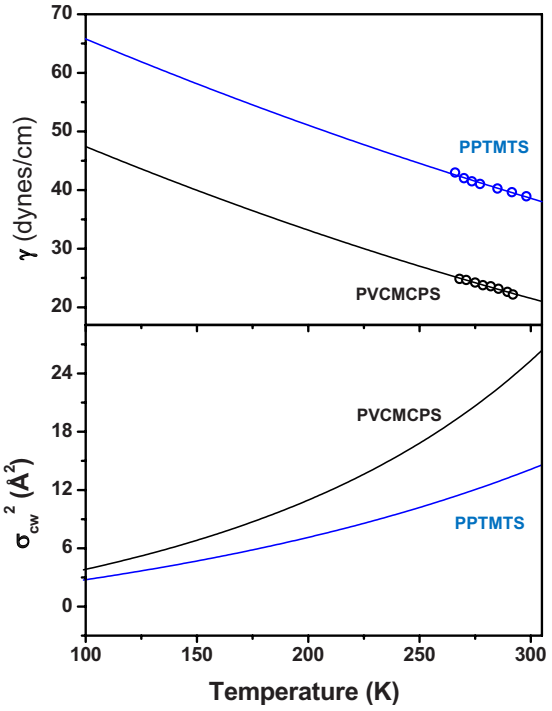

FIG. 2. (Color online) The upper panel shows the temperature dependence of the surface tension (γ) for PPTMTS and PVPMCPS: circles indicate data obtained using a Wilhelmy-plate method in the range 265–298 K, and solid lines show the fitted and then extrapolated γ using $\ln(\gamma)=A+n\ln(T_c-T)$, where A and n are constants, and T_c is the critical temperature of the liquid. The lower panel shows the calculated σ_{cw}^2 vs T for PPTMTS and PVPMCPS.

results due to sample preparation. The thickness is much larger than relevant length scales (surface roughness, molecular dimensions, etc.). The substrates used were etched using hydrofluoric acid such that the rms surface roughness is >20 Å. This ensures that scattering from the internal interface, which is not of interest here, contributes only a very diffuse signal and is easily removed through the conventional process of subtracting the off-specular background.[20,28] Before deposition of PPTMTS films, the cleaned Si wafers were etched once again with 2% HF to make the substrates hydrophobic, which allowed us to get uniform wetting. This step was not required for PVCMCPS. We detected no measurable changes in film thickness and its wetting properties (or uniformity) over at least 3 days for PPTMTS and at least 1 day for PVCMCPS, which confirms that the evaporation rate is very low and film is stable.

Specular x-ray reflectivity studies were performed using a conventional four-circle diffractometer. The beam size was ~0.5 mm vertically and ~1 mm horizontally, and the momentum resolution was ~0.004 $Å^{-1}$. The samples were mounted on the cold head of a closed-cycle refrigerator and covered with a beryllium radiation shield, which helps to keep the sample temperature uniform. The cold head and the sample were then sealed under vacuum with a beryllium can. The whole system was pumped with a molecular turbo pump to maintain a vacuum. Before collecting data, the sample was kept at the desired temperature for at least 30 min for the system to reach equilibrium. In addition to specular scans,

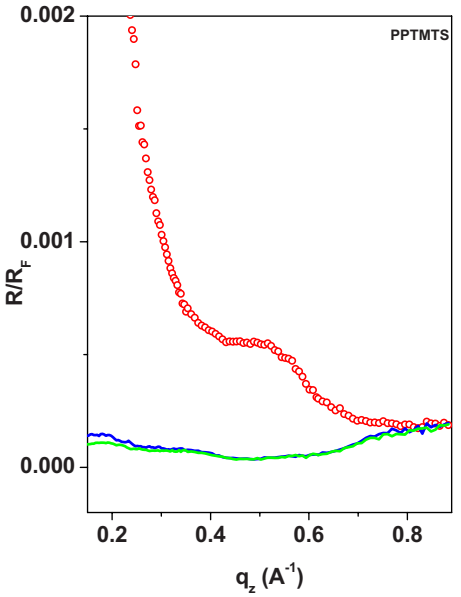

FIG. 3. (Color online) Specular reflectivity data (circles) before background subtraction, divided by the Fresnel reflectivity R_F, for PPTMTS at 235 K. R_F is the theoretical reflectivity from an ideal surface. The two solid lines show slightly off-specular data (sample misaligned by $\pm 0.1°$).

slightly off-specular "background" scans were performed and subtracted from the specular data, thus removing the scattering from all diffuse sources including that from the rough liquid-solid interface. Figure 3 shows the specular reflectivity R divided by the Fresnel reflectivity R_F (before background subtraction) along with two corresponding off-specular scans at 235 K for PPTMTS. The specular scan (open circle) shows a clear "hump" centered around 0.5 Å^{-1}, which is completely absent in off-specular scans (solid lines). This indicates that the structure in the specular reflectivity is significant and not part of the off-specular background.

The background-subtracted reflectivity data were fitted using the distorted crystal model, frequently used to fit reflectivity data from liquid-metal surfaces.[12,26] It consists of a semi-infinite series of Gaussians with increasing widths. As with the liquid metals Bi and Sn, we found that there is a density enhancement at the surface that requires us to modify the model to include two regions with different average densities. Thus we assume that there is a density of the form

$$\frac{\rho(z)}{\rho_{\text{bulk}}} = r\sum_{n=0}^{n=1} \frac{d_0}{\sqrt{2\pi}\sigma_n} e^{-(z-nd_0)^2/2\sigma_n^2} + \sum_{n=2}^{\infty} \frac{d_1}{\sqrt{2\pi}\sigma_n} e^{-[z-(n-2)d_1-2d_0]^2/2\sigma_n^2},$$

where $\sigma_n^2 = \sigma_0^2 + n\bar{\sigma}^2 = \sigma_i^2 + \sigma_{\text{cw}}^2 + n\bar{\sigma}^2$. In other words the width of the first layer is σ_0, and subsequent layer widths increase at a rate that depends on the magnitude of $\bar{\sigma}$. The first layer width σ_0 is further decomposed into an intrinsic term σ_i due to all noncapillary factors and a term σ_{cw} due to thermal capillary waves. The first two layers have a different density

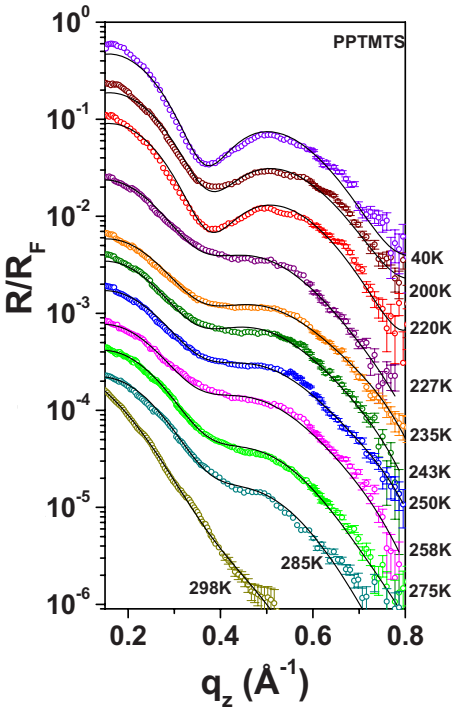

FIG. 4. (Color online) Specular reflectivity data (divided by R_F) for PPTMTS films on rough silicon substrates, at different temperatures. Lines are the best fits from which the electron-density profiles are determined.

(multiplicative factor r) and a different spacing (d_0) compared to subsequent layers (spacing d_1): note that this form for the density has no specific physical justification; it is used because it is easier to integrate, because the trends in the parameters are informative (see below), and because its consistent use allows the behavior of different liquids to be compared (we will compare some of these at the end of this paper). Note also that σ_{cw} is not a variable fitting parameter; it is calculated from extrapolated surface tension data, as mentioned earlier in the context of Fig. 2.

III. RESULTS: PPTMTS

We recently reported[22] that liquid PPTMTS shows a sharp increase in the persistence of the surface layers into the bulk materials at its glass transition temperature ($T_g \sim 224$ K). Here we show additional details regarding the temperature-dependent trends. Figure 4 shows the specular reflectivity R divided by the Fresnel reflectivity R_F at selected temperatures. At 298 K, the scans are featureless. At lower temperatures, distinct reflectivity oscillations are seen, indicating that there is some structure in the density profile, in particular the hump centered around 0.5 Å^{-1} mentioned above. This increase in intensity allows data to be collected to higher q_z at temperatures below 298 K. These changes imply changes in the surface electron density $\rho(z)$ averaged over the plane. The change in the reflectivity data appears at the same temperature whether we are going up or down and does not have any detectable dependence on age or temperature history of the sample, x-ray exposure, etc. The temperature threshold is

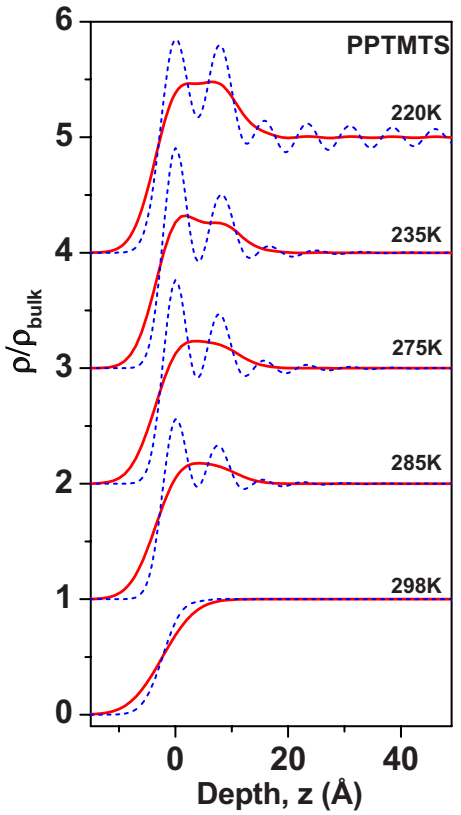

FIG. 5. (Color online) Electron-density profiles of PPTMTS films on rough silicon substrates, at selected typical temperatures. Solid lines (red) show best fit normalized electron densities $[\rho(z)/\rho_{\text{bulk}}]$. The dashed lines (blue) show the density profiles with capillary broadening removed (i.e., plotted with $\sigma_{\text{cw}}=0$). The profiles have been shifted vertically for clarity.

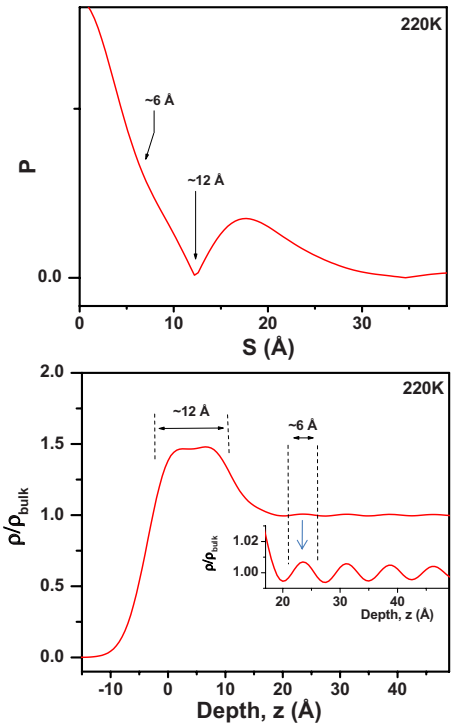

FIG. 6. (Color online) Top: Patterson function and bottom: electron-density profile obtained using the distorted crystal model at 220 K for PPTMTS. A section of the profile is also shown enlarged. The vertical dashed lines in the bottom panel indicate the internal interfaces in the liquid, the distances between which correspond to minima and maxima in the Patterson function.

~285 K, which is only slightly below room temperature and much higher than the threshold for TEHOS (~230 K). However, in terms of T_c, it corresponds to $T/T_c \approx 0.23$, the same as for TEHOS and close to that seen in recent simulations.[17]

Figure 5 shows typical fitted electron densities $\rho(z)$ in five temperature regions. The solid lines are the actual best-fit electron-density profiles; the dashed lines are the same density functions, except with $\sigma_{\text{cw}}=0$. In other words, the dashed lines show what the surface profiles would look like if they had not been broadened by thermal capillary waves. The temperature-dependent density profiles show the emergence of surface density oscillations with decreasing temperature, with a threshold at 285 K, i.e., $\sim 0.23T_c$. (This was clear even in the raw reflectivity data, discussed in context of Fig. 4).

Figure 6 shows the Patterson function of the $R(q)/R_F(q)$ data at temperature 220 K, which is compared with the extracted electron-density profile using the distorted crystal model. The Patterson function is model-independent: a maximum or minimum in the Patterson function at a given s indicates that there are two interfaces a distance s apart; if the density is changing in the same direction at both interfaces, there will be a maximum, while if one is increasing and the other is decreasing, there will be a minimum. Figure 6 shows the Patterson function and extracted electron-density profile nicely correspond to each other, which indicates that the basic conclusions regarding the electron-density profile are independent of the model used.

Figure 7 shows the trends in some fitting parameters for PPTMTS. The surface-density enhancement factor r (Fig. 7, top left) shows only a weak and featureless temperature dependence. The layer spacings d_0 and d_1 are shown in the bottom-left panel of Fig. 7, and these are essentially temperature-independent. The average values of d_0 and d_1 are 7.8 Å and 7.5 Å, respectively. The top surface roughness, σ_0 (Fig. 7, top right) decreases with decreasing temperature in the layered liquid phase, as expected because the roughness is due in part to thermal capillary waves. Near and below T_g there is some variability but the roughness does not increase very sharply at the transition. It should be noted here that σ_i, the intrinsic top surface roughness after subtracting the roughness due to capillary waves, remains constant (~2.2 Å) in the layered PPTMTS liquid above T_g.[22] The parameter $\bar{\sigma}$ is shown in bottom-right panel of Fig. 7. The horizontal lines are guides to the eye. There is an abrupt change in $\bar{\sigma}$ by a factor of 2 at the glass transition, indicating that the layers penetrate further into the bulk when $T<T_g$. This trend was already observed qualitatively in Fig. 4, where reflectivity data show a sudden shape change (or it becomes much sharper) below T_g. See Ref. 22 for further discussion of this effect, which constitutes the first observation of a structural change at a liquid-glass transition.

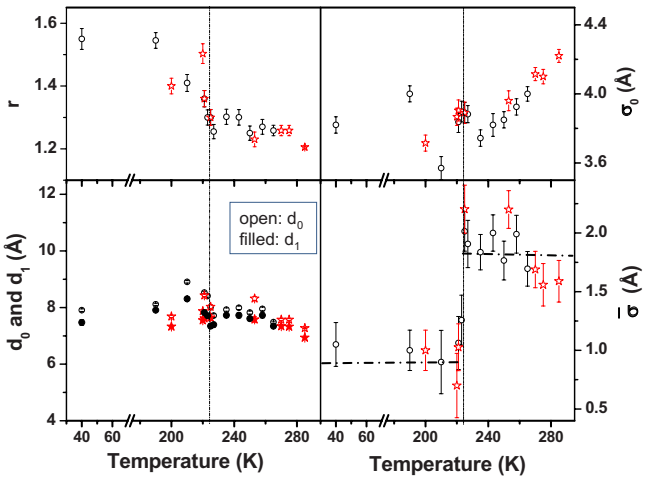

FIG. 7. (Color online) Temperature dependence of the fitting parameters for PPTMTS. Symbols indicate the temperature history of the sample (○: temperature was lowered to the value shown; ☆: temperature was increased to the value shown). Top left: surface-density enhancement parameter r. Bottom left: d_0 (open symbols) and d_1 (filled symbols), the spacings between the first three layers and between subsequent layers, respectively. Top-right: σ_0, the top surface roughness, bottom-right: $\bar{\sigma}$, which measures how rapidly the layers broaden as one goes into the bulk. The dotted vertical lines show T_g as measured in Ref. 29. The horizontal dashed lines are guides to the eye.

IV. RESULTS: PVPMCPS

Figure 8(a) shows the specular reflectivity (R/R_F) for PVPMCPS at various temperatures. At 150 K, the scans are featureless. At lower temperatures, distinct reflectivity oscillations are seen, indicating that there is some structure in the reflectivity. The temperature threshold is at ~128 K, much

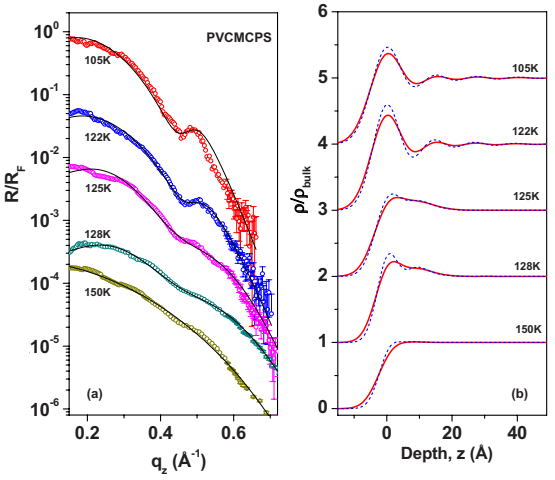

FIG. 8. (Color online) (a) Specular reflectivity data (divided by R_F) of PVPMCPS films on rough silicon substrates. Lines are best fits. (b) The corresponding electron-density profiles. Solid lines (red) show best fit normalized electron densities $[\rho(z)/\rho_{\text{bulk}}]$. The dashed lines (blue) show the density profiles with capillary broadening removed (i.e., plotted with $\sigma_{\text{cw}}=0$). The profiles have been shifted vertically for clarity.

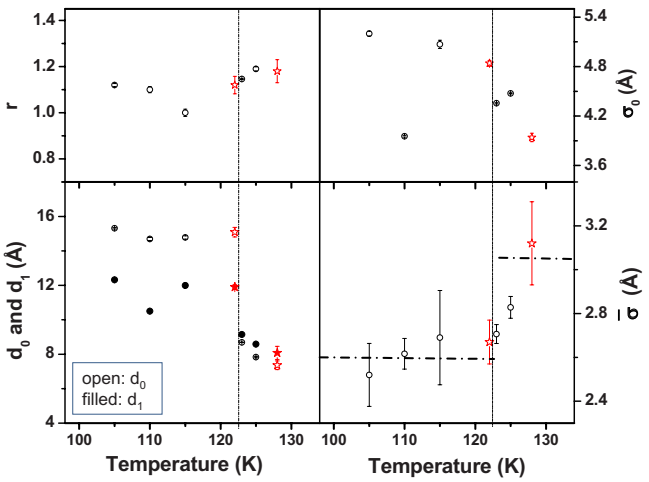

FIG. 9. (Color online) Temperature dependence of the fitting parameters for PVPMCPS. Symbols indicate the temperature history of the sample (○: temperature was lowered to the value shown; ☆: temperature was increased to the value shown). Top left: surface-density enhancement parameter r. Bottom left: d_0 (open symbols) and d_1 (filled symbols), the spacing between the first three layers and between subsequent layers, respectively. Top right: σ_0, the top surface roughness. Bottom right: $\bar{\sigma}$, which measures how rapidly the layers broaden as one goes into the bulk.

lower than the threshold for PPTMTS (~285 K), and TEHOS (~230 K).[20] In terms of T_c, it corresponds to $T/T_c \approx 0.17$, not the same value as for PPTMTS and TEHOS,[20] but still in the neighborhood of 0.20. At the onset of surface layering, the surface tension of these three dielectric liquids PVPMCPS, PPTMTS, and TEHOS are ~42 dyn/cm, ~40 dyn/cm, and ~37 dyn/cm, respectively (see Fig. 2 and Ref. 21).

Figure 8(b) shows the fitted electron densities at the same five selected temperatures as in Fig. 8(a). The solid lines are the actual best-fit electron density profiles; the dashed lines are the same density functions, except with $\sigma_{\text{cw}}=0$. Three major features should be noted in Fig. 8(b). First, it is clear that surface oscillations appear at 128 K and below. Second, there is a density hump at the surface when the oscillations appear. A similar effect is seen in PPTMTS, TEHOS,[20] Sn,[9] and Bi.[30] However, it is not seen in simulations[17] and is not predicted theoretically.[10] This surface-density enhancement is discussed further in Ref. 30. Third, at and below 122 K, the layer spacing (d_0 and d_1) increases compared to the values at higher temperatures. There is also a qualitative difference at and below 122 K: the oscillations are larger and persist further into the bulk material.

Figure 9 shows the trends in some fitted parameters. The surface-density enhancement r shows no specific trend with temperature (Fig. 9, top left). As mentioned in earlier section, the layer spacings (d_0 and d_1, Fig. 9, bottom left) increase with decreasing temperature. Above 122 K, the average values of d_0 and d_1 were ~8 Å and ~7.5 Å, respectively, but at and below 122 K d_0 and d_1 increase to ~15 and ~12 Å. These molecules are quite flexible and the changes can reasonably be attributed to changes in molecular conformation near the interface. σ_0 and $\bar{\sigma}$ are shown in Fig. 9, top-right

and bottom-right panels, respectively. The trend in σ_0 is similar to, and probably attributable to, the trend in the layer spacings. However, $\bar{\sigma}$ appears to change sharply at 122 K although the data above 122 K are limited. (The range of temperatures between 122 K and the layering onset temperature of 130 K is quite small.) We speculate that the temperature 122 K is the glass transition temperature for PVPMCPS. The direct measurement of mechanical properties at this low temperature is difficult and has not yet been performed for this material.

Note that no solidlike diffraction peaks have been observed for PVPMCPS or PPTMTS at any temperature. Below 105 K, for PVPMCPS, we observe only featureless reflectivity profiles, probably due to increased surface roughness (σ_0) at lower temperatures (see the trend in Fig. 9, top right).

V. DISCUSSION

The fact that the layering threshold (in simulations and molecular liquids) is consistently around $0.2T_c$ is an empirical result, but the use of scaled temperatures (T/T_c) is reasonable on general grounds. Early predictions of layered surface structures[2,31] suggested that the surface profile would be monotonic only at T_c and oscillatory elsewhere. Subsequently, Evans *et al.*[32] pointed out that the density profile at an interface would mimic the long-range decay of the two-point correlation function $g(r)$: when this is oscillatory, there will be surface layers, and when it is monotonic, the surface density will be also. The relationship between $g(r)$ and the density as a function of distance from the interface follows from mean-field (density-functional) considerations. The Fisher-Widom line[33] (in, e.g., the p-T plane) separates states with oscillatory vs decaying asymptotic $g(r)$. Unfortunately the asymptotic behavior of $g(r)$ is not accessible to experiments on atomic/molecular liquids. Evans *et al.* calculated that the Fisher-Widom line crosses the liquid-vapor coexistence curve at $0.9T_c$, which means that most liquid surfaces will be layered in room-temperature experiments. As we know, this is not so. Subsequently, Tarazona *et al.*[34] calculated that the Fisher-Widom line can be at much lower temperatures (as low at $0.32T_c$) depending on the pair potential.

Thus while the Fisher-Widom line may define a rigorous upper limit to where layers might be observed, it does not necessarily tell us where the layers actually are observed in practice. Moreover, there might not be a sudden transition at the Fisher-Widom line, since oscillations in $g(r)$ should develop slowly as T is lowered, and if so the same slow development should be seen in surface-density oscillations. Even if it is postulated that layers become visible at temperatures much lower than the Fisher-Widom line because of the obscuring effect of surface fluctuations, the surface tension changes slowly with temperature. Therefore the sudden onset of layers at $\sim 0.2T_c$, although a reproducible physical phenomenon in multiple systems, remains unexplained.

Are surface ordering in liquid metals and surface ordering in dielectric liquids the same phenomenon, or two entirely different physical effects that coincidentally have similar experimental manifestations? Certainly any explanation for dielectric liquids should also apply to liquid metals (although not vice versa). Parsimony (Occam's razor) argues for a single explanation but this does not constitute proof. There is no liquid identical to (say) mercury except for being nonmetallic, or identical to (say) PPTMTS except with conduction electrons. Even if it were possible to safely heat mercury to $0.23T_c$ ($\sim$400 K) and do x-ray reflectivity there, thermal fluctuations (capillary waves) are likely to prevent the phenomenon from being observed there.[35] Other liquid metals have even higher predicted thresholds.

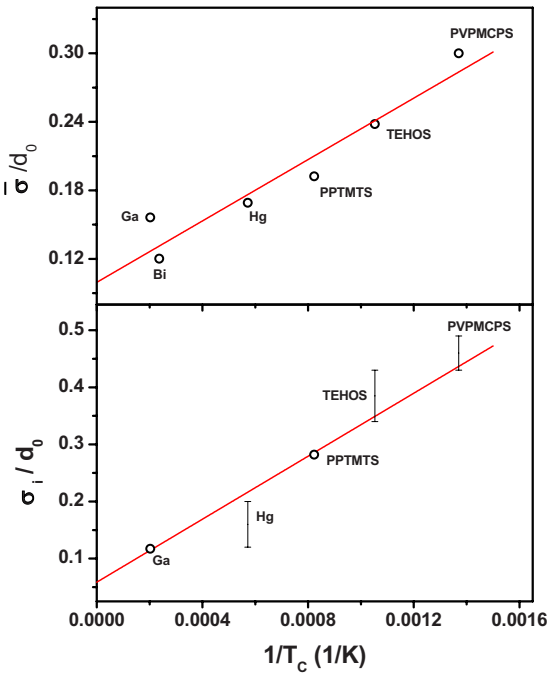

FIG. 10. (Color online) T_c dependence of some surface-layering parameters for different isotropic liquids. The width parameters have been divided by the layer spacing in the same material to obtain scale-independent parameters so that atomic and molecular liquids can be compared. The lines are guides to the eye.

However, there are some clues that there may be a common mechanism. One argument that could be made in favor of different origins for metallic vs nonmetallic layering is that the layering "peak" in our TEHOS data is significantly weaker than in Hg or Ga. (Of course, many liquid metals[14,30] have peaks weaker than Hg or Ga.) Both liquid-metal and dielectric liquid-layering data have been analyzed with the distorted-crystal model. Since the length scale (e.g., the layer spacing or the atomic/molecular size) varies significantly between molecular vs elemental materials, $\bar{\sigma}$ and σ_i have been divided by d_0, the layer spacing, to create the scale-independent variables plotted in Fig. 10. Since $\bar{\sigma}$ does not appear to have a significant temperature dependence in any given material in the layered liquid phase,[12,15,20–22,30] available values have been used irrespective of the temperature at which they were measured. Figure 10, top panel shows the plot of $\bar{\sigma}/d_0$ for different dielectric and metallic liquids, showing surface layering,[12,15,21,30] with their defined or estimated[24,36,37] critical temperature (T_c). In and Sn, which also have surface layers, are not shown because their T_c is not known. Note that for Bi we have used the $\bar{\sigma}/d_0$ data from

Ref. 30. They have shown series of $\bar{\sigma}$ values depending on the other fitting parameters. We have chosen the best fit value of $\bar{\sigma}/d_0$ (where σ_A, the width of the top adlayer, is ~0.5 Å). The plot shows a roughly linear relationship of $\bar{\sigma}/d_0$ with $1/T_c$. Similarly σ_i/d_0 shows a roughly linear dependence on $1/T_c$ (Fig. 10, bottom panel). Bi is not shown in this plot because the value of σ_i is not given in Ref. 30. For some of these liquids σ_i/d_0 is observed to vary slightly with the experimental temperature: for these liquids the vertical line indicates the range.

Remarkably, the materials with higher $\bar{\sigma}$ and σ_i values have smaller T_c so that both metal and dielectric data fall on the same curves (Fig. 10). In terms of $1/T_c$, there is a roughly linear trend. We speculate that longer-range interatomic/intermolecular interactions could be responsible for higher T_c and also for stronger layering. These graphs suggest that layering was seen first in liquid metals not only because they are "cold" even at room temperature, but because their longer-range interactions give rise to stronger layer ordering at their free surfaces (thus making the effect easy to observe). This has led to the possibly unjustified impression that liquid metals are unique.

In the 1970s and early 1980s, there was a large amount of theoretical and simulation activity in the area of liquid surface structure, but the corresponding level of experimental capabilities did not exist. The situation is largely reversed today. The availability of synchrotron radiation has dramatically improved our ability to "see" the liquid surface. We hope that the phenomena reported here will soon be explained theoretically and that this will lead to a better understanding of the liquid state.

ACKNOWLEDGMENTS

This work was supported by the U.S. National Science Foundation under Grant No. DMR-0705137. We used the facilities of the Center for Functional Nanomaterials (CFN), Beam Line X-18A at the National Synchrotron Light Source (NSLS) and Sector 33-BM-C at the Advanced Photon Source (APS), all of which are supported by the U.S. Department of Energy.

[1] "Nouvelle théorie de l'action capillaire," S. D. Poisson, Bachelier, Paris (1831).
[2] For example, Clive A. Croxton, *Liquid State Physics: A Statistical Mechanical Introduction* (Cambridge University Press, Cambridge, 1974).
[3] L. B. Lurio, T. A. Rabedeau, P. S. Pershan, F. Isaac, Silvera, M. Deutsch, S. D. Kosowsky, and B. M. Ocko, Phys. Rev. Lett. **68**, 2628 (1992).
[4] B. M. Ocko, X. Z. Wu, E. B. Sirota, S. K. Sinha, and M. Deutsch, Phys. Rev. Lett. **72**, 242 (1994).
[5] M. K. Sanyal, S. K. Sinha, K. G. Huang, and B. M. Ocko, Phys. Rev. Lett. **66**, 628 (1991).
[6] W. Zhao, X. Zhao, J. Sokolov, M. H. Rafailovich, M. K. Sanyal, S. K. Sinha, B. H. Cao, M. H. Kim, and B. B. Sauer, J. Chem. Phys. **97**, 8536 (1992).
[7] W. Zhao, M. H. Rafailovich, J. Sokolov, L. J. Fetters, R. Plano, M. K. Sanyal, S. K. Sinha, and B. B. Sauer, Phys. Rev. Lett. **70**, 1453 (1993).
[8] A. Braslau, M. Deutsch, P. S. Pershan, A. H. Weiss, J. Als-Nielsen, and J. Bohr, Phys. Rev. Lett. **54**, 114 (1985).
[9] O. Shpyrko, M. Fukuto, P. S. Pershan, B. M. Ocko, I. Kuzmenko, T. Gog, and M. Deutsch, Phys. Rev. B **69**, 245423 (2004).
[10] M. P. D'Evelyn and S. A. Rice, Phys. Rev. Lett. **47**, 1844 (1981).
[11] M. P. D'Evelyn and S. A. Rice, J. Chem. Phys. **78**, 5081 (1983).
[12] O. M. Magnussen, B. M. Ocko, M. J. Regan, K. Penanen, P. S. Pershan, and M. Deutsch, Phys. Rev. Lett. **74**, 4444 (1995); M. J. Regan, E. H. Kawamoto, S. Lee, P. S. Pershan, N. Maskil, M. Deutsch, O. M. Magnussen, B. M. Ocko, and L. E. Berman, *ibid.* **75**, 2498 (1995); H. Tostmann, E. DiMasi, P. S. Pershan, B. M. Ocko, O. G. Shpyrko, and M. Deutsch, Phys. Rev. B **59**, 783 (1999).
[13] E. DiMasi, H. Tostmann, O. G. Shpyrko, M. Deutsch, P. S. Pershan, and B. M. Ocko, J. Phys. Condens. Matter **12**, A209 (2000).
[14] O. G. Shpyrko, P. Huber, A. Grigoriev, P. Pershan, B. Ocko, H. Tostmann, and M. Deutsch, Phys. Rev. B **67**, 115405 (2003).
[15] O. G. Shpyrko, A. Y. Grigoriev, C. Steimer, P. S. Pershan, B. Lin, M. Meron, T. Graber, J. Gerbhardt, B. Ocko, and M. Deutsch, Phys. Rev. B **70**, 224206 (2004).
[16] B. Yang, D. Gidalevitz, D. Li, Z. Huang, and S. A. Rice, Proc. Natl. Acad. Sci. U.S.A. **96**, 13009 (1999); B. Yang, D. Li, Z. Huang, and S. A. Rice, Phys. Rev. B **62**, 13111 (2000); B. Yang, D. Li, and S. A. Rice, *ibid.* **67**, 212103 (2003).
[17] E. Chacón, M. Reinaldo-Falagán, E. Velasco, and P. Tarazona, Phys. Rev. Lett. **87**, 166101 (2001).
[18] E. Velasco, P. Tarazona, M. Reinaldo-Falagán, and E. Chacón, J. Chem. Phys. **117**, 10777 (2002).
[19] D. Li and S. A. Rice, J. Phys. Chem. **108**, 19640 (2004).
[20] H. Mo, G. Evmenenko, S. Kewalramani, K. Kim, S. N. Ehrlich, and P. Dutta, Phys. Rev. Lett. **96**, 096107 (2006).
[21] H. Mo, S. Kewalramani, G. Evmenenko, K. Kim, S. N. Ehrlich, and P. Dutta, Phys. Rev. B **76**, 024206 (2007).
[22] S. Chattopadhyay, A. Uysal, B. Stripe, G. Evmenenko, S. Ehrlich, E. A. Karapetrova, and P. Dutta, Phys. Rev. Lett. **103**, 175701 (2009).
[23] *A User's Guide to Vacuum Technology*, 2nd ed., edited by J. F. O'Hanlon (Wiley, New York, 1989), p. 242.
[24] K. M. Klincewicz and R. C. Reid, AIChE J. **30**, 137 (1984).
[25] For example, J. Maroto, F. J. de las Nieves, and M. Quesada-Perez, Eur. J. Phys. **25**, 297 (2004).
[26] E. DiMasi, H. Tostmann, B. M. Ocko, P. S. Pershan, and M. Deutsch, Phys. Rev. B **58**, R13419 (1998).
[27] F. P. Buff, R. A. Lovett, and F. H. Stillinger, Phys. Rev. Lett. **15**, 621 (1965)
[28] C. J. Yu, A. G. Richter, J. Kmetko, S. W. Dugan, A. Datta, and P. Dutta, Phys. Rev. E **63**, 021205 (2001).

[29] C. Maggi, B. Jacobsen, T. Christensen, N. B. Olsen, and J. C. Dyre, J. Phys. Chem. B **112**, 16320 (2008).
[30] P. S. Pershan, S. E. Stoltz, G. O. Shpyrko, M. Deutsch, V. S. K. Balagurusamy, M. Meron, B. Lin, and R. Streitel, Phys. Rev. B **79**, 115417 (2009).
[31] G. M. Nazarian, J. Chem. Phys. **56**, 1408 (1972).
[32] R. Evans, J. R. Henderson, D. C. Hoyle, A. O. Parry, and Z. A. Sabeur, Mol. Phys. **80**, 755 (1993).
[33] M. E. Fisher and B. Widom, J. Chem. Phys. **50**, 3756 (1969).
[34] P. Tarazona, E. Chacon, and E. Velasco, Mol. Phys. **101**, 1595 (2003).
[35] M. J. Regan, P. S. Pershan, O. M. Magnussen, B. M. Ocko, M. Deutsch, and L. E. Berman, Phys. Rev. B **54**, 9730 (1996).
[36] *CRC Handbook of Chemistry and Physics*, 90th ed. (CRC Press, Philadelphia, PA 2009); A. A. Likalter, J. Phys.: Condens. Matter **3**, 2795 (1991).
[37] D. K. Belashchenko and O. I. Ostrovskii, Russ. J. Phys. Chem. **80**, 509 (2006).